Catal Lett (2007) 119:134–141
DOI 10.1007/s10562-007-9210-x

Pt-Al_2O_3 Cryogel with High Thermal Stability for Catalytic Combustion

Toshihiko Osaki · Kiho Nagashima · Koji Watari · Koji Tajiri

Received: 5 June 2007 / Accepted: 9 July 2007 / Published online: 25 July 2007

Abstract The cryogel catalyst of platinum on alumina was prepared from aluminum sec-butoxide and H_2PtCl_6 through the sol-gel technique and subsequent freeze drying. The cryogel catalyst showed higher thermal stability of platinum than the corresponding xerogel or impregnation catalysts, which was ascribed to the more intimately developed platinum-alumina interaction accompanied by the encapsulation of the metal into the alumina cryogel. It was also shown that platinum accessibility was higher on the cryogel than on the xerogel despite the higher thermal stability of the metal on the formed than on the latter. For the VOC combustion, the cryogel exhibited higher activity than the xerogel and impregnation catalysts. Also for the methane combustion the cryogel showed higher activity, although it showed lower activity than the impregnation catalysts above 600 °C. By the addition of ceria as an additive to the cryogel catalyst, the CH_4 combustion activity was improved especially in the temperature region above 600 °C.

Keywords Cryogel · Sol-gel · Freeze drying · Platinum · Alumina · Catalytic combustion · Thermal stability · Dispersion · VOC · Methane

1 Introduction

Platinum-alumina catalysts have been prepared by a conventional impregnation or an ion-exchange method, applicable to the catalytic combustion of hydrocarbons [1]. The sol-gel technique has also been applied to synthesize the catalyst from a homogeneous solution of the metal and support precursors, by which high metal dispersion throughout the alumina support was achieved [2–5]. Furthermore, by employing supercritical drying as a drying method for the wet gel, the collapsed of the gel network could be suppressed, resulting in the aerogels with very low bulk density. On such aerogels, sintering and coking were successfully prevented as well as improving the activity and stability at high temperatures [6]. However, the aerogels did not always show superior properties by comparison to the corresponding xerogels. Balakrishnan and Gonzalez prepared aerogel and xerogel catalysts of platinum-alumina systems, and concluded that the aerogels were inferior in comparison to the corresponding xerogels as far as the surface area and metallic dispersion were concerned [7]. The comparison of aerogel and xerogel catalysts were also done by Courtheoux et al. [8] and Popa et al. [9]; for the catalytic propellant decomposition the aerogels showed lower activities, although they had superior properties compared with xerogels. Sault et al. developed a platinum-alumina aerogel catalyst via a combination of inverse micelle technology with sol-gel processing [10]; although the aerogel exhibited higher turnover frequency for propane dehydrogenation than the xerogel, the Pt diameter and the BET surface area were much larger and smaller, respectively, for the aerogels. Aside from the aspect of these inferior properties compared to the xerogels, the commercial application of aerogels seems very limited because of the high cost in production. The supercritical drying should be the most costly process because of employing high pressures in an autoclave. The drying at high pressures is hazardous and furthermore, there is possibility of not only effluence of platinum ions

---

T. Osaki (✉) · K. Nagashima · K. Watari · K. Tajiri
National Institute of Advanced Industrial Science and Technology (AIST), 2266-98, Anagahora, Shimoshidami, Moriyama-ku, Nagoya 463-8560, Japan
e-mail: t-osaki@aist.go.jp

from wet gels but also uncontrolled reduction to metallic platinum during the drying and/or solvent exchange.

Cryogels, the highly porous solid materials derived from wet gels through freeze drying, are fascinating and useful in that they possess the bulk density as very low as that of aerogels [11, 12]. The drying is safer, more economical, and there is very little fear of the effluence of platinum ions and uncontrolled reduction during the drying. The solvent exchange is also unnecessary if the gel is prepared in an aqueous solution. Despite the simple drying method, very few studies have been performed on the preparation and catalysis of noble metals-alumina cryogels so far [11, 13]. In this paper, platinum-alumina cryogel was prepared by one-step addition of Pt precursor before gelation and subsequent removal of solvent via freeze drying, and the thermal stability of platinum and catalytic activity were investigated by comparison to those of the corresponding xerogel and impregnation catalysts.

2 Experimental

Aluminum sec-butoxide (0.029 mol, Kanto Chemicals) was hydrolyzed with ultra-pure water (20 mL) in a flask at 86 °C, and the resultant mixture was kept with stirring for a while. Then 1.0 mol L^{-1} nitric acid (4.0 mL, Wako Pure Chemicals) was added to the sol for peptization and the sol was refluxed for a few hours with stirring to obtain clear boehmite sol. On the other hand, 0.37 g of H_2PtCl_6 aqueous solution (2.0 wt.%, Tanaka Precious Metals) was mixed with the aqueous solution (4.8 mL) containing oxalic acid (0.088 mol L^{-1}, Wako Pure Chemicals) and ammonia (0.60 mol L^{-1}, Wako Pure Chemicals), and the solution was kept at 86 °C for 30 min. The platinum solution was then introduced to the boehmite sol and the mixture was refluxed at 86 °C with vigorous stirring. For gelation, urea (0.2 g, Wako Pure Chemicals) was added to the sol, and the sol was allowed to stand for one night at 86 °C. The gel obtained was frozen at a liquid nitrogen temperature without the solvent exchange, and subsequently dried under vacuum on a laboratory freeze-drier (Tokyo-Rikakikai, FDU-810) equipped with a vacuum pump (Ulvac, GCD-051X), with a condenser. The dried gel was calcined in air in the temperature range of 500–800 °C. The platinum content was 0.5 wt.% on a weight base. For comparison, the wet gel was dried under the normal drying conditions to obtain a xerogel catalyst. The impregnation catalysts were prepared by a conventional impregnation method using pure alumina cryogel (287 m^2 g^{-1}) prepared by the method described above without Pt, and commercial alumina (Taimei Kagaku, TM-300D; 200 m^2 g^{-1}) as the catalyst supports. For simplifying the description, the impregnation catalyst using the alumina cryogel is denoted hereafter as Imp(cryo), whereas that using the commercial alumina is as Imp(com).

Crystalline phases were identified using an X-ray powder diffractometer (Rigaku, RAD-1VC) at 30 kV and 30 mA with a Cu tube. Transmission electron micrographs (TEM) were taken on a JEOL 2010 instrument operated at the accelerating voltage of 200 kV. The CO gas adsorption on catalysts was measured by a conventional pulse technique using helium as a carrier gas. The BET (Brunauer–Emmett–Teller) surface area, pore volume, and mean pore size were measured on a volumetric N_2-gas adsorption measurement instrument (Nippon BEL, Belsorp-mini) at a liquid nitrogen temperature.

The catalytic combustion of VOC containing acetaldehyde, methanol, and methyl formate was carried out using a continuous flow reactor at atmospheric pressure. The catalyst (0.01 g) calcined at 500 °C for 1 h followed by reduction with pure hydrogen (30 mL min^{-1}) at 500 °C for 1 h was diluted with quartz sand (0.99 g), and then placed in a quartz reactor (ϕ = 8 mm, i.d.), followed by admitting the mixed reactants (CH_3CHO: 67 ppm, HCO_2CH_3: 33 pm, and CH_3OH: 33 ppm in air; 99 mL min^{-1}) in the temperature range of 50–400 °C. The effluent gases were analyzed by an FID gas chromatography (Shimadzu, GC-14B) with a separation of column of Shin-carbon A. The catalytic combustion of methane was performed as follows: the catalyst (0.1 g) calcined at 700 °C for 1 h followed by reduction at 500 °C for 1 h was diluted with quartz sand (0.9 g), and placed in the quartz reactor. Then, the reactant gases (CH_4: 1%, O_2: 20%, Ar: 79%; 100 mL min^{-1}) were admitted into the reactor in the temperature range of 400–700 °C. The effluent gases were analyzed by an FID gas chromatography (Shimadzu, GC-14A) with a separation column of DC-200.

3 Results

Figure 1 shows the BET surface area, pore volume and mean pore size of the catalysts. The surface area was larger for the cryogel, xerogel and Imp(cryo) than for Imp(com); among the former three catalysts the difference was not significant. The surface area decreased with increasing the calcination temperature for all the catalysts. As for the pore volume, it was larger for Imp(cryo) than for other catalysts; the value of ca. 440 mm^3 g^{-1} was kept until 700 °C calcination for Imp(cryo) suggesting the textural resistance, whereas at 500 °C the volume was almost the same as that of the cryogel. The mean pore size became large with calcination temperature for the xerogel and Imp(cryo), whereas it was not markedly changed for the cryogel.

Figure 2 shows XRD profiles of the catalysts after the calcination in the temperature range of 500–800 °C. The Pt

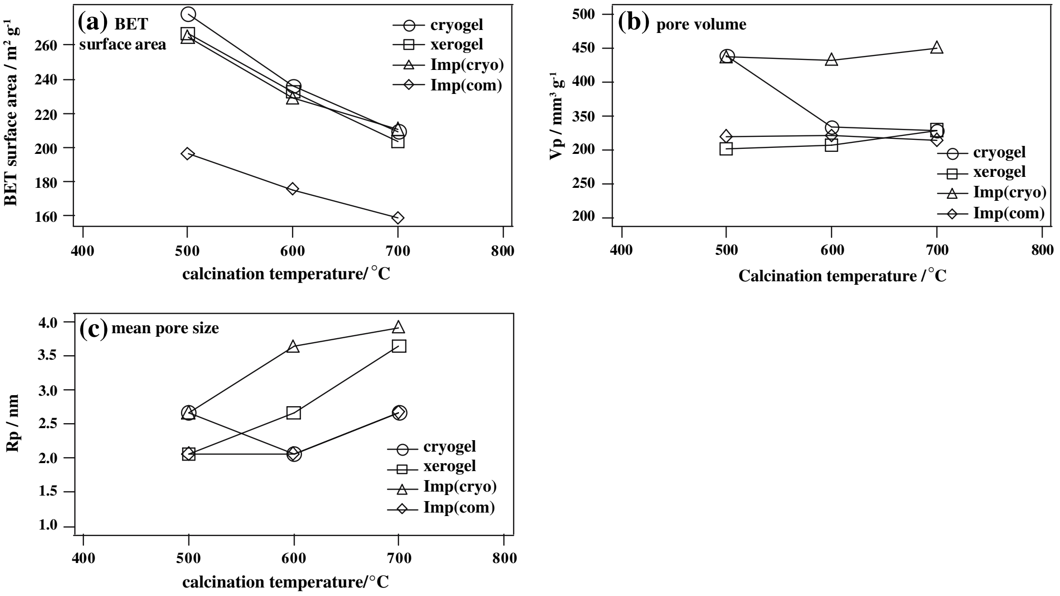

Fig. 1 (**a**) BET surface area, (**b**) pore volume, and (**c**) mean pore size of the catalysts after the calcination for 1 h; ○: cryogel, □: xerogel, Δ: Imp(cryo), and ◇: Imp(com). The pore volume and mean pore size were calculated by the BJH (Barret–Joyner–Halenda) method

peak was not observed on all the catalysts after the calcination at 500 °C. Calcination at 600 °C resulted in the appearance of metallic Pt diffraction peaks on Imp(com), indicating the sintering of platinum. By employing alumina cryogel as a catalyst support for impregnation, the thermal stability was markedly improved; i.e., the peak was observed above 750 °C calcination on Imp(cryo), indicating the shift to 150 °C higher temperature. On the xerogel, the Pt diffraction peak was observed at 800 °C, but not on the cryogel at the temperature, suggesting further

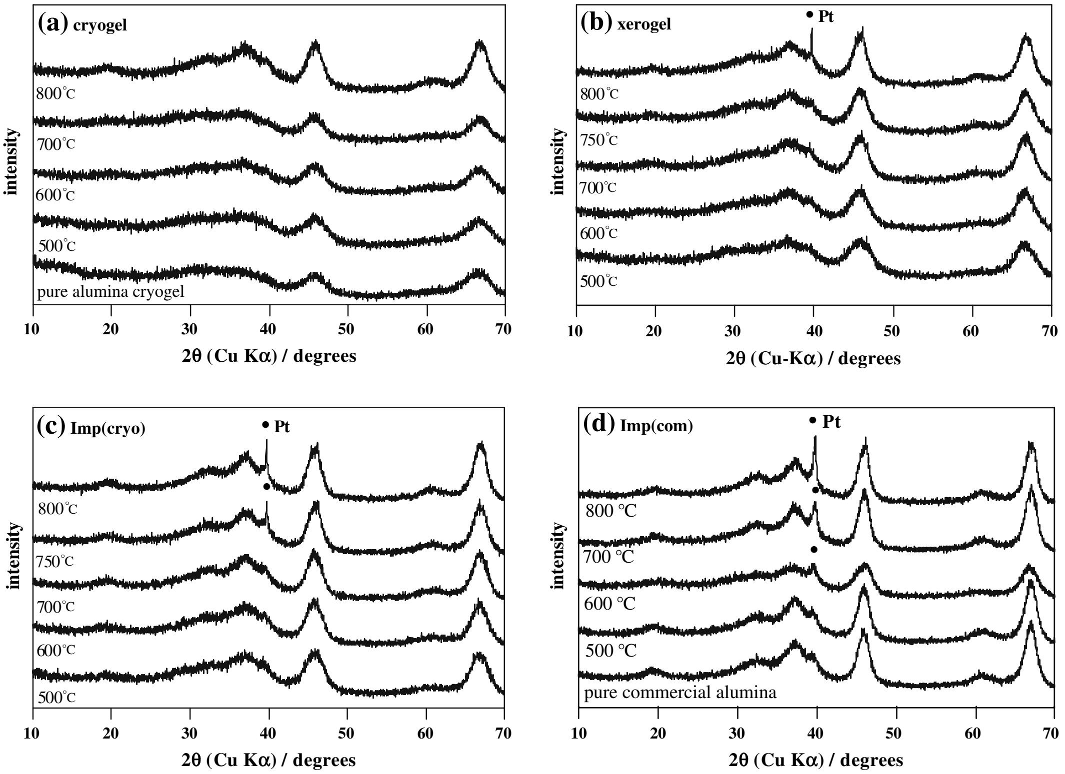

Fig. 2 XRD patterns of the catalysts after the calcination for 2 h; (**a**) cryogel, (**b**) xerogel, (**c**) Imp(cryo), and (**d**) Imp(com)

improvement of the thermal stability of platinum by employing sol-gel technique and subsequent freeze drying.

TEM images of the catalysts after the calcination at 700 °C are shown in Fig. 3. The platinum particles were not observed on the cryogel and xerogel after the calcination, whereas on Imp(cryo) Pt nanoparticles with the diameter of ca. 1 nm were seen. On Imp(com), sintered Pt particles over 20 nm were observed. After the calcination followed by reduction with hydrogen at 500 °C, such nanoparticles appeared also on the cryogel and xerogel (Fig. 4); the particle size was almost the same (ca. 1 nm) between the two sol-gel catalysts of cryogel and xerogel. As for the Imp(cryo), the nanoparticles appeared more pronouncedly after the reduction than before. Whereas such fine particles were not observed on Imp(com) even after the reduction. After the calcination of the catalysts at 800 °C, sintered large particles over 50 nm were seen also on the xerogel and Imp(cryo), but not on the cryogel, suggesting higher thermal stability of platinum on the cryogel, the results of which were in agreement with those of XRD shown in Fig. 2.

Results of chemisorption of CO on the catalysts after the calcination in the temperature range of 500–700 °C are shown in Fig. 5. At 500 °C calcination, the chemisorption was lower on the cryogel and xerogel catalysts than on the impregnation catalysts. Upon increasing the calcination temperature, the chemisorption number decreased markedly on the impregnation catalysts. Between the two impregnation catalysts, the decrease was more significant on Imp(com) than on Imp(cryo). Whereas such significant decrease was not observed on the cryogel and xerogel catalysts. Between the two sol-gel catalysts, the chemisorption number was larger on the cryogel than on the xerogel; the amount on the cryogel was ca. 1.5–2 times as large as that on the xerogel in all the temperature range examined.

Figure 6 shows the results of catalytic combustion of VOC on the catalysts. For all the VOC, the cryogel exhibited the highest combustion activity, whereas the xerogel showed the lowest. Between the two impregnation catalysts, the activity was higher on Imp(cryo) than on Imp(com), although the difference was not significant for methyl formate combustion.

Figure 7 shows the catalytic combustion of methane over the catalysts. The cryogel, xerogel and Imp(cryo) showed higher activity than Imp(com) below 550 °C; among the former three catalysts, the activity was slightly higher on the cryogel than on other catalysts, although the difference was very small. Whereas above 600 °C, the activity was higher on Imp(com) than on other catalysts, indicating the change of the order of combustion activity around 550–600 °C.

4 Discussions

4.1 Thermal Stability of Platinum

In a previous study, the thermal stability of alumina cryogels at high temperatures was investigated to reveal the

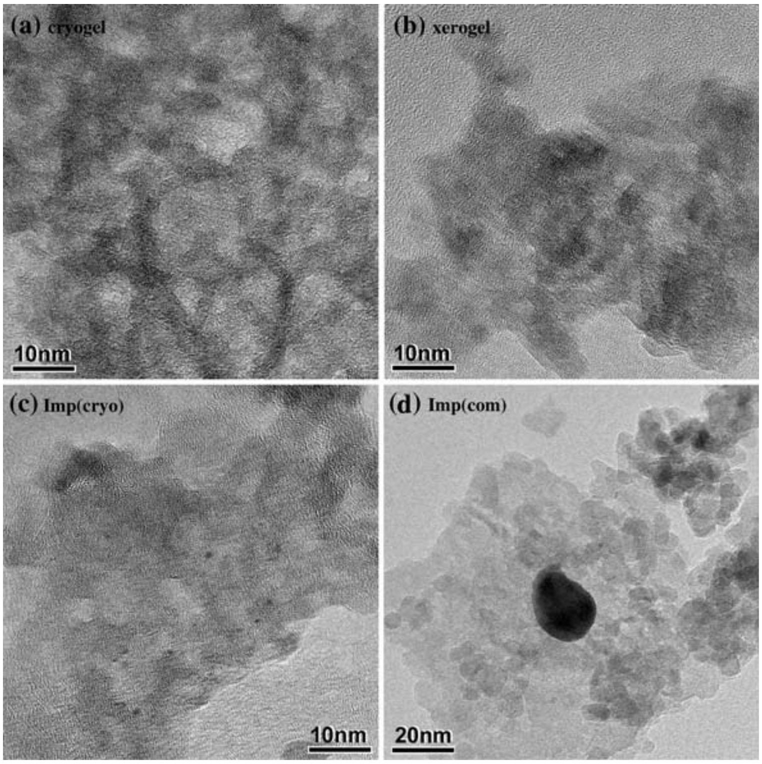

Fig. 3 TEM images of the catalysts after the calcination at 700 °C for 2 h; (**a**) cryogel, (**b**) xerogel, (**c**) Imp(cryo), and (**d**) Imp(com)

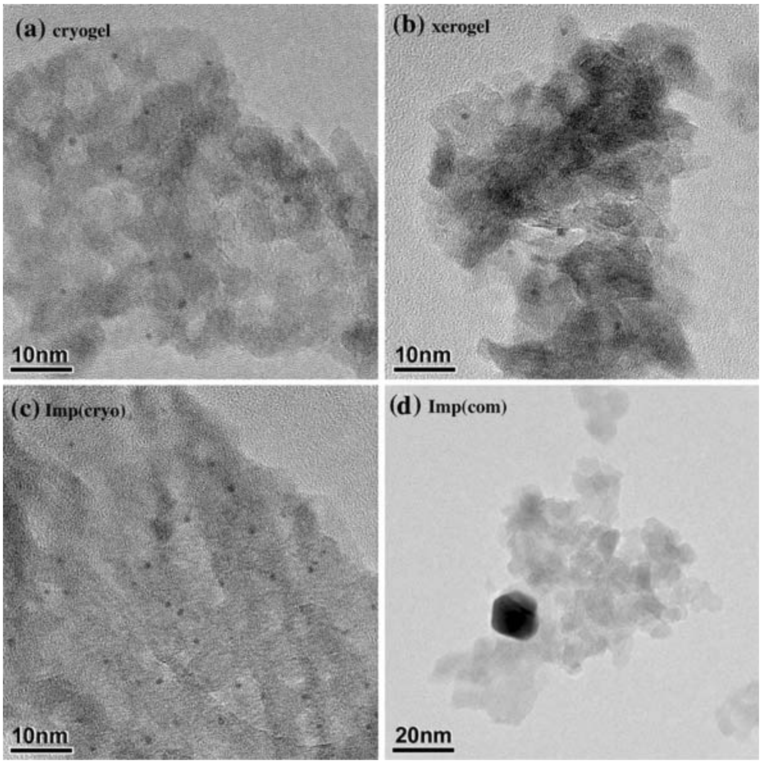

Fig. 4 TEM images of the catalysts after the calcination at 700 °C for 1 h followed by the reduction at 500 °C for 1 h; (**a**) cryogel, (**b**) xerogel, (**c**) Imp(cryo), and (**d**) Imp(com)

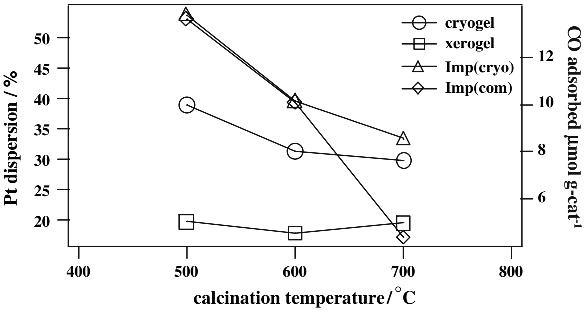

Fig. 5 Platinum dispersion after the calcination for 1 h followed by the reduction at 500 °C for 1 h; ○: cryogel, □: xerogel, Δ: Imp(cryo), and ◇: Imp(com)

performance as a catalyst support [12]. It was found that the pure alumina cryogel (the apparent density: ca. 0.05 g cm^{-3}) exhibited higher stability than the corresponding xerogel (ca. 1.0 g cm^{-3}), alumina precipitate (ca. 0.8 g cm^{-3}), and commercial alumina (ca. 0.4 g cm^{-3}) due to the much lower apparent density of the cryogel as very low as that of aerogel. It was also revealed that the addition of a certain portion of silica to the alumina cryogel resulted in further improvement of thermal stability. In the present study, the stability of platinum on alumina was examined. From the results of XRD and TEM observations, the thermal stability of platinum can be summarized as the following order: cryogel > xerogel > Imp(cryo) > Imp(com). It is generally known that platinum can disperse as oxide on the Al_2O_3 surface at temperatures below the decomposition temperatures of the oxide, i.e., ca. 585 °C or even higher temperatures if the complex between the platinum oxide and the support surface possesses sufficient stability [14]. It is also known that the sintering of platinum is followed by the decomposition of platinum oxide to metallic platinum [14, 15]. On Imp(com) the sintering was observed at 600 °C calcination (Fig. 2), in good agreement with the temperature mentioned above. The observed higher thermal stability of platinum on the cryogel, xerogel, and Imp(cryo) than on Imp(com) can be ascribed to the alumina gel support synthesized from aluminum alkoxide through the sol-gel processing. Among the former three catalysts, the cryogel and xerogel showed the higher stability than the Imp(cryo) despite the very little difference of BET surface area (Fig. 1). It is known for the sol-gel catalysts that precious metals are incorporated into the framework of the support [16, 17], or partially buried at the surface of the support [18, 19]. In the present study, platinum particles could not be observed by TEM after the calcination on the cryogel and xerogel catalysts (Fig. 3), whereas CO chemisorption was smaller on these sol-gel catalysts than on the Imp(cryo) catalyst (Fig. 5). These results strongly suggest that very fine platinum oxide are highly dispersed and partially buried in the alumina gels after the calcination, and such encapsulation is considered the principal cause for the higher thermal stability of platinum on the sol-gel catalysts at high temperatures.

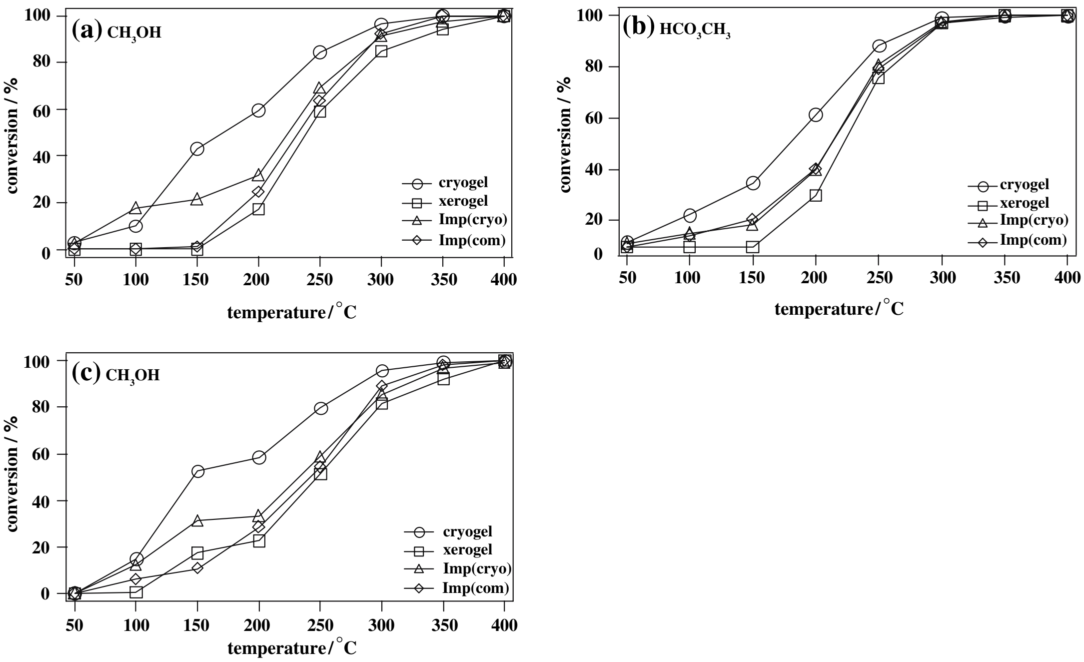

Fig. 6 The activity for the combustion of (**a**) acetaldehyde, (**b**) methyl formate, and (**c**) methanol on the catalysts; ○: cryogel, □: xerogel, Δ: Imp(cryo), and ◇: Imp(com). The catalysts were calcined at 500 °C for 1 h followed by the reduction at 500 °C for 1 h

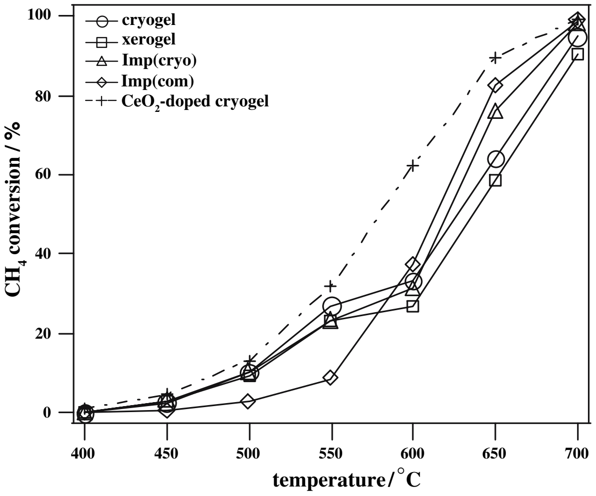

Fig. 7 The CH_4 combustion activity on the catalysts; ○: cryogel, □: xerogel, Δ: Imp(cryo), ◇: Imp(com), and +: 10 wt.% CeO_2-doped cryogel. The catalysts were calcined at 700 °C for 1 h followed by the reduction at 500 °C for 1 h

It is interesting to notice that, between the two sol-gel catalysts, CO chemisorption was higher on the cryogel than on the xerogel despite that platinum stability was also higher on the former than on the latter. The stability of platinum may be derived from the encapsulation as explained above and therefore, the metal accessibility and its thermal stability are considered in a trade-off relationship. The higher stability of platinum on the cryogel might be a result of more intimately developed interaction between the highly dispersed platinum and alumina support [20], brought about through the freeze drying of wet co-gel. Or the alumina cryogel as a catalyst support, having higher thermal stability than the corresponding xerogel, might also contribute to the stability of platinum to some degree. Assuming here that the mean diameter of Pt particles is 1 nm for both cryogel and xerogel (Fig. 4), the theoretical Pt dispersion, D_M, is calculated to be ca. 73% from the following Anderson's equation [21]:

$$d_{VA} = \alpha(M_w/a_m \rho N_0)(1/D_M)$$

where d_{VA} is a mean particle diameter of Pt, α is a geometrical parameter, M_W is the atomic weight of Pt, a_m is the effective area occupied by a Pt atom in the surface, ρ is the density, and N_0 is Avogadro's number. In the present study, α was taken as 6 on the assumption of the spherical particles, and a_m was taken as 12.5 nm^{-2} according to the literature [22]. If all of the platinum were outside the gel, the dispersion of ca. 73% be obtained. As shown in Fig. 5, however, the observed Pt dispersion at 700 °C was ca. 30 and 20% on the cryogel and xerogel, respectively. By comparison with these calculated and observed values, it can roughly be deduced that ca. 59 and 73% of platinum surface were inside the alumina gel for the cryogel and xerogel, respectively. In the xerogel catalyst, platinum may be buried more firmly inside the alumina gel due to the remarked shrinkage of wet gel during the normal drying and thereby, such lower metal accessibility might be observed. In addition, Pt ions in the wet gel may be moved during the evaporation of water and therefore, the lower thermal stability of platinum might be observed. Further studies are still necessary for unambiguous discussions.

It should also be noted that the thermal stability of platinum on an impregnation catalyst was remarkably improved by employing alumina cryogel as a catalyst support (Figs. 2 and 3). The Pt dispersion after 700 °C calcination was higher on Imp(cryo) (33%) than on Imp(com) (17%), in agreement with the results of XRD and TEM. The higher thermal stability can be attributed to not only the larger surface area of alumina cryogel but also its high water-durability. The cryogel was highly durable in water despite having the apparent density as very low as that of aerogel in addition to being thermally stable at elevated temperatures [12]. Therefore, the structural and textural properties of the alumina cryogel should be maintained even after the impregnation followed by the treatment in air at high temperatures. The pore volume of Imp(cryo), which was larger than that of other catalysts, was almost unchanged by the calcination temperature (Fig. 1), suggesting the superiority of alumina cryogel support also for impregnation.

4.2 Catalytic Activities

From the results of catalytic VOC combustion shown in Fig. 6, the activity was found in the order of cryogel > Imp(cryo) ≥ Imp(com) ≥ xerogel. TEM observations revealed that Pt nanoparticles with ca. 1 nm diameter were present on all the catalysts, and no sintered particles were seen under the pretreatment conditions. Whereas CO chemisorption under the pretreatment conditions was in the order of Imp(cryo) ≈ Imp(com) > cryogel > xerogel (Fig. 5), which implies that the combustion activity order can not be explained only by the number of the active sites. On the cryogel the platinum particles might be more active due to the higher concentration of active sites such as kink or step. Or the alumina cryogel support might also contribute to the combustion activity, i.e., the polar molecules of CH_3CHO, CH_3OH, and HCO_2CH_3 are adsorbed not only on Pt metals but also on the cryogel support or the metal-support boundary, also on which the combustion reaction might proceed. Whereas on the xerogel having the lowest CO chemisorption among the catalysts examined, the catalytic activity was also the lowest, which suggests that the number of active sites is nevertheless one of the important factors to understand the VOC combustion activity qualitatively.

On the other hand, the activity order for CH_4 combustion, the molecule of which is nonpolar, was different from that for VOC. The combustion activity was in the order of cryogel ≥ xerogel ≈ Imp(cryo) > Imp(com) below 550 °C, whereas of Imp(com) > Imp(cryo) ≥ cryogel > xerogel above 600 °C, indicating the change of the order of activity around 550–600 °C. The CO chemisorption under the pretreatment conditions was Imp(cryo) > cryogel > xerogel ≥ Imp(com) (Fig. 5), which implies that the activity order can not be understood only from the number of active sites as in the case of VOC. TEM observations revealed that fine Pt particles with ca. 1 nm diameter were observed on the cryogel, xerogel, and Imp(cryo), whereas sintered large particles over 20 nm on Imp(com) under the pretreatment conditions (Fig. 4), it might be considered that fine particles are preferable for CH_4 combustion in the low temperature region, whereas large particles in the high temperature region. It is reported that the propane combustion activity decreased with increasing the Pt dispersion over the catalyst supported on metal oxides [23, 24]. This implies that the reaction is structure-sensitive, i.e., the larger platinum particles are favorable for the propane combustion. In the present methane combustion, however, the larger particles seemed to be favorable only in the high temperature region above 600 °C. Taking into account the fact that the methane conversions were relatively insensitive to changes in the temperature around 550–600 °C on the cryogel, xerogel and Imp(cryo), but not on the Imp(com), the observed activity order change might be attributed to the physical and/or chemical properties of alumina gel support rather than to those of platinum. Further examinations are still necessary for revealing the true factors. In Fig. 7, the catalytic activity of the cryogel with CeO_2 as an additive was also shown. When ceria was introduced to the cryogel, the activity was improved especially in the temperature region above 600 °C. This improvement may primarily be ascribed to the ability of ceria for storing oxygen and stabilizing platinum dispersion, as the oxide has been employed for automotive emission control as a standard additive of three way catalysts [25, 26]. Recent spectroscopic analyses have revealed that platinum was stabilized by ceria through the strong bond of Pt–O–Ce as an anchor [27], by which the sintering of platinum was successfully suppressed. By optimizing the ceria content, further improvement is expected.

5 Conclusions

Pt-Al_2O_3 cryogel, prepared by the sol-gel processing and subsequent freeze drying, showed higher thermal stability of platinum than the corresponding xerogel and impregnation catalysts. The higher stability was considered as a result of the stronger interaction between platinum and alumina through the encapsulation of the metal into the cryogel; i.e., about half of the platinum surface was considered to be inside the cryogel. It was also shown that the cryogel had high activity for catalytic combustion of VOC and methane. Taking into account the simple and safe drying process with low cost, the resultant cryogel seems more fascinating for industrial applications as combustion catalysts than the aerogel derived from supercritical drying.

References

1. Ishikawa A, Komai S, Satsuma A, Hattori T, Murakami Y (1994) Appl Catal A-Gen 110:61
2. Cho IH, Park SB, Cho SJ, Ryoo R (1998) J Catal 173:295
3. Dolev A, Shter GE, Grader GS (2003) J Catal 214:146
4. Castillo S, Moran-Pineda M, Molina V, Gomez R, Lopez T (1998) Appl Catal B-Environ 15:203
5. Manasilp A, Gulari E (2002) Appl Catal B-Environ 37:17
6. Mizushima Y, Hori M (1992) Appl Catal A-Gen 88:137
7. Balakrishnan K, Gonzalez RD (1993) J Catal 144:395
8. Courtheoux L, Popa F, Gautron E, Rossignol S, Kappenstein C (2004) J Non-Cryst Solids 350:113
9. Popa AF, Courtheoux L, Gautron E, Rossignol S, Kappenstein C, Euro J Inorg Chem (2005) 543
10. Sault AG, Martino A, Kawola JS, Boespflug E (2000) J Catal 191:474
11. Pajonk GM (1997) Catal Today 35:319
12. Osaki T, Nagashima K, Watari K, Tajiri K (2007) J Non-Cryst Solids 353:2436
13. Kirchnerova J, Klvana D, Chaouki J (2000) Appl Catal A-Gen 196:191
14. Prasad R, Kennedy LA, Ruckenstein E (1984) Catal Rev-Sci Eng 26:1
15. Lieske H, Lietz G, Spindler H, Volter J (1983) J Catal 81:8
16. Lopez T, Romero A, Gomez R (1991) J Non-Cryst Solids 127:105
17. Bosch P, Lopez T, Lara VH, Gomez R (1993) J Mol Catal 80:299
18. Azomoza M, Lopez T, Gomez R, Gonzalez RD (1992) Catal Today 15:547
19. Lopez T, Bosch P, Moran M, Gomez R (1993) J Phys Chem 97:1671
20. Schneider M, Duff DG, Mallat T, Wildberger M, Baiker A (1994) J Catal 147:500
21. Anderson JR (1975) Structure of metallic catalysts. Academic Press, London p 359
22. Anderson JR (1975) Structure of metallic catalysts. Academic Press, London p 296
23. Yazawa Y, Yoshida H, Hattori T (2002) Appl Catal A-Gen 237:139
24. Matsuhashi H, Nishiyama S, Miura H, Eguchi K, Hasegawa K, Iizuka Y, Igarashi A, Katada N, Kobayashi J, Kubota T, Mori T, Nakai K, Okazaki N, Sugioka M, Umeki T, Yazawa Y, Lu DL (2004) Appl Catal A-Gen 272:329
25. Yao HC, Yao YFY (1984) J Catal 86:254
26. Komai S, Yazawa Y, Satsuma A, Hattori T (2005) J Jpn Petrol Inst 48:173
27. Nagai Y, Hirabayashi T, Dohmae K, Takagi N, Minami T, Shinjoh H, Matsumoto S (2006) J Catal 242:103